The Effect of Ionic Defect Interactions on the Hydration of Yttrium-doped Barium Zirconate

Article Supplement

Sebastian Eisele,[1] Fabian M. Draber,[2] and Steffen Grieshammer[3]

[1] *Sebastian Eisele (s.eisele@fz-juelich.de)*
Helmholtz-Institut Münster (IEK-12), Forschungszentrum Jülich GmbH, Corrensstr. 46, 48149 Münster, Germany.
Institute of Physical Chemistry, RWTH Aachen University, Landoltweg 2, 52056 Aachen, Germany.
[2] *Fabian M. Draber (draber@pc.rwth-aachen.de)*
Institute of Physical Chemistry, RWTH Aachen University, Landoltweg 2, 52056 Aachen, Germany.
[3] *Steffen Grieshammer (s.grieshammer@fz-juelich.de)*
Helmholtz-Institut Münster (IEK-12), Forschungszentrum Jülich GmbH, Corrensstr. 46, 48149 Münster, Germany.
Institute of Physical Chemistry, RWTH Aachen University, Landoltweg 2, 52056 Aachen, Germany.

ABSTRACT

This supplement extends the main article "The Effect of Ionic Defect Interactions on the Hydration of Yttrium-doped Barium Zirconate". The pair interaction models calculated with density functional theory are quantified for the short-range and long-range cases, including symmetry reduced geometries and energies. Information on the applied in-house Monte Carlo software MOCASSIN concerning the Metropolis annealing routine is provided. Additionally, the results using the long-range interaction model for BZY10, BZY20, and BZY30 not contained in the main article, the derivation for the mass action law as applied in the main article, the derivation of the calculation of F from MMC results, and $\Delta F'_{\mathrm{int}}$ raw data tables are provided.

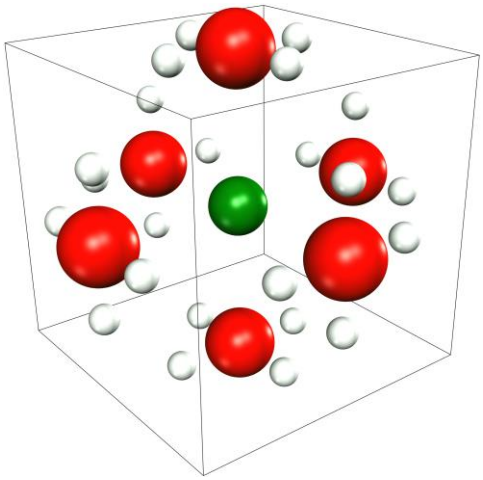

1 BZO structure

The exact BZO unit cell description used for the MMC simulations and in the following pair interaction tables is summarized in Table 1. The affiliated space group of the perovskite BZO is $Pm\bar{3}m$ (No. 221) with 48 symmetry operations and the unit cell parameter is 4.23 Å. The undoped barium sites were omitted during simulation and the chosen $H_i^{\bullet}$ site is at 1.00 Å distance to the oxygen site.

Table 1. The non-idealized BZO unit cell as used for the pair interaction description.

Site	Pos. A	Pos. B	Pos. C	N	Possible Species	Species Distribution
Zr	0.5000	0.5000	0.5000	1	Zr_{Zr}^{x}, Y'_{Zr}	Random
O	0.5000	0.5000	0.0000	3	$O_O^x, v_O^{\bullet\bullet}$	MMC equilibration
H_i	0.7636	0.5000	0.0000	12	$v_i^x, H_i^{\bullet}$	MMC equilibration
Ba	0.0000	0.0000	0.0000	1	Ba_{Ba}^{x}	Omitted in MMC

2 Pair interaction models

The applied DFT interaction models use pair interactions for the MMC active species that are defects in the ideal BZO host matrix; namely, oxygen vacancy $v_O^{\bullet\bullet}$, interstitial proton $H_i^{\bullet}$, and yttrium ion Y'_{Zr}. The $Y'_{Zr} - Y'_{Zr}$ interactions were not modelled

as the Zr sublattice occupants were uniformly distributed at random prior to the simulations. No MMC equilibration of the cation sublattice was conducted and thus the $Y'_{Zr} - Y'_{Zr}$ interactions had no influence on the results. The relevant interactions are summarized in Table 2 to Table 6. Here, interactions with ID values containing an "a,b,c,..." label mark interactions at the same distance but with different reference geometries, and IDs extended with a second "1,2,3,..." label mark interactions at the same distance where the affiliated extended vector sets in the unit cell are chiral to each other. This means, they cannot be fully mapped onto each other by the space group symmetry operations without an additional chirality-breaking operation and it is not possible to calculate distinct values for the two sets using DFT. Each table has a fixed occupation pair, a fixed site for the first position and a variable position for the second site. Geometric data is provided as (a,b,c) coordinates in the affine coordinate system of the unit cell. The last three columns of the tables define the number of interactions per site after P1 translation of the symmetry reduced structure for the origin site (#Origin) and the partner site (#Partner), and the model affiliations with (S) for short-range and (L) for long-range model, respectively. The last decimal for each energy value is uncertain.

2.1 Interactions between yttrium and oxygen vacancies

Table 2. The $Y_{Zr} - v_O^{\bullet\bullet}$ interaction data with the Zr_{Zr}^x origin site at (0.5 0.5 0.5). Last decimal of energy values is uncertain.

ID	Distance / Å	Partner Site Position (a, b, c)			Energy / eV	#Origin	#Partner	Model
1	2.1150	0.0000	0.5000	0.5000	-0.362	6	2	S, L
2	4.7293	-0.5000	0.0000	0.5000	-0.276	24	8	S, L
3-a	6.3450	-0.5000	-0.5000	0.0000	-0.068	24	8	L
3-b	6.3450	-1.0000	0.5000	0.5000	-0.068	6	2	L

2.2 Interactions between yttrium and interstitial protons

Table 3. The $Y_{Zr} - H_i^{\bullet}$ interaction data with the Zr_{Zr}^x origin site at (0.5 0.5 0.5). Last decimal of energy values is uncertain.

ID	Distance / Å	Partner Site Position (a, b, c)			Energy / eV	#Origin	#Partner	Model
1	2.3395	0.0000	0.2636	0.5000	-0.298	24	2	S, L
2	3.8608	-0.2636	0.0000	-0.5000	-0.366	24	2	S, L

2.3 Interactions between oxygen vacancies

Table 4. The $v_O^{\bullet\bullet} - v_O^{\bullet\bullet}$ interaction data with the O_O^x origin site at (0.5 0.5 0.0). Last decimal of energy values is uncertain.

ID	Distance / Å	Partner Site Position (a, b, c)			Energy / eV	#Origin	#Partner	Model
1	2.9911	0.0000	0.5000	0.5000	0.237	8	8	S, L
2-a	4.2300	0.5000	0.5000	0.0000	-0.092	4	4	S, L
2-b	4.2300	0.5000	0.5000	-1.0000	2.293	2	2	S, L

2.4 Interactions between oxygen vacancies and interstitial protons

Table 5. The $v_O^{\bullet\bullet} - H_i^{\bullet}$ interaction data with the O_O^x origin site at (0.5 0.5 0.0). Last decimal of energy values is uncertain.

ID	Distance / Å	Partner Site Position (a, b, c)			Energy / eV	#Origin	#Partner	Model
1	1.0000	0.2636	0.5000	0.0000	2.569	4	1	S, L
2	2.3909	0.0000	0.5000	0.2636	0.006	8	2	S, L
3	3.1538	0.0000	0.2636	0.5000	-0.072	16	4	S, L
4	3.2300	-0.2636	0.5000	0.0000	-0.188	4	1	S, L

5	3.7651	0.0000	0.5000	0.7364	0.139	8	2	S, L
6-a	4.3466	-0.5000	0.2636	0.0000	-0.032	8	2	L
6-b	4.3466	0.2636	0.5000	-1.0000	-0.032	8	2	L
7	4.4022	-0.2636	0.0000	-0.5000	-0.024	16	4	L
8	4.8590	-0.5000	0.0000	-0.2636	-0.018	16	4	L

2.5 Interactions between interstitial protons

Table 6. The $H_i^{\cdot} - H_i^{\cdot}$ interaction data with the $\varnothing_i^x$ origin site at (0.7364 0.5 0.0). Last decimal of energy values is uncertain.

ID	Distance / Å	Partner Site Position (a, b, c)			Energy / eV	#Origin	#Partner	Model
1	1.4142	0.5000	0.2636	0.0000	1.212	2	2	S, L
2	1.5768	1.0000	0.5000	-0.2636	0.176	2	2	S, L
3	2.0000	0.2636	0.5000	0.0000	2.342	1	1	S, L
4	2.2300	1.2636	0.5000	0.0000	-0.143	1	1	S, L
5-1	2.5916	0.5000	0.0000	0.2636	-0.040	4	4	S, L
5-2	2.5916	1.0000	0.2636	-0.5000	-0.040	4	4	S, L
6	2.9911	0.7364	0.0000	0.5000	-0.058	4	4	S, L
7-1	3.3085	0.0000	0.5000	0.2636	0.064	2	2	S, L
7-2	3.3085	1.0000	0.5000	-0.7364	0.064	2	2	S, L
8-1	3.3813	0.5000	-0.2636	0.0000	0.008	2	2	S, L
8-2	3.3813	1.5000	0.2636	0.0000	0.008	2	2	S, L
9	3.5981	0.2636	0.0000	0.5000	-0.037	4	4	S, L
10	3.7309	1.2636	0.0000	-0.5000	0.119	4	4	S, L
11-1	3.8957	0.0000	0.2636	0.5000	0.003	4	4	S, L
11-2	3.8957	0.5000	0.0000	0.7364	0.003	4	4	S, L
12-1	4.0186	1.0000	-0.2636	-0.5000	0.028	4	4	S, L
12-2	4.0186	1.5000	0.0000	-0.2636	0.028	4	4	S, L
13-a-1	4.2300	-0.2636	0.5000	0.0000	0.040	1	1	S, L
13-a-2	4.2300	1.7364	0.5000	0.0000	0.040	1	1	S, L
13-b	4.2300	0.7364	-0.5000	0.0000	0.170	2	2	S, L
13-c	4.2300	0.7364	0.5000	-1.0000	0.477	2	2	S, L
14	4.4053	0.0000	0.5000	0.7364	0.229	2	2	L
15	4.4631	0.5000	0.2636	-1.0000	0.346	4	4	L
16	4.5143	1.0000	-0.5000	-0.2636	0.057	4	4	L
17	4.5679	1.5000	-0.2636	0.0000	0.110	2	2	L
18-a	4.6790	0.2636	-0.5000	0.0000	0.000	2	2	L
18-b	4.6790	0.2636	0.5000	-1.0000	0.369	2	2	L
19-a	4.7818	1.2636	-0.5000	0.0000	0.130	2	2	L
19-b	4.7818	1.2636	0.5000	-1.0000	0.130	2	2	L
20-1	4.9608	0.0000	-0.2636	-0.5000	0.023	4	4	L
20-2	4.9608	1.5000	0.0000	-0.7364	0.023	4	4	L

3 Monte Carlo routine & software

The Metropolis Monte Carlo (MMC) simulations where performed with our in-house software MOCASSIN[1] ("Monte Carlo for Solid State Ionics"). To model the temperature changes in the annealing routine, the usual Boltzmann probability *P*

defining the probability of changing from one system state to another was modified with a factor $\alpha(T)$ as shown in expression (1). Here, T_{min} is the minimal target temperature and T is the current temperature. In this formalism, $\alpha = 0$ and $\alpha = 1$ represent infinite temperature T_{∞} and the final temperature $\mathrm{T_{min}}$, respectively, and the solver gradually simulates $\alpha[0 \rightarrow 1]$ for one system. A description of the implementation can be found in the affiliated publication.

$$P = \exp\left(\frac{\Delta E \cdot \alpha(T)}{k_{\mathrm{B}} T_{\mathrm{min}}}\right) \text{ with } \alpha(\mathrm{T}) = \frac{\mathrm{T_{min}}}{T} \tag{1}$$

A minimal C pseudocode implementation of the distribution recording routine is illustrated in Code 1. Here, the 'DoMmcCycle(...)' function refers to the usual MMC cycle processing the supplied alpha according to expression (1).

Code 1. Minimal C pseudocode of the MMC annealing routine that logs MMC distributions. The SITE_BLOCKED flag signals that no transition rule was found, these cases are omitted from the total counts so that only ACCEPTED and REJECTED attempts are recorded.

```
for (alpha = 0; alpha <= 1.0; alpha += alphaStep)
{
	for (i = 0; i < preRunAttemptCount; i++)
	{
		while (DoMmcCycle(simulation, alpha) != SITE_BLOCKED) {}
	}

	for (i = 0; i < mainRunAttemptCount; i++)
	{
		while (DoMmcCycle(simulation, alpha) != SITE_BLOCKED) {}
		WriteInternalEnergyToDistribution(simulation, distribution);
	}
	WriteDistributionToDatabase(distribution);
	ResetDistribution(distribution);
}
```

4 Results of the long-range interaction model

4.1 Results for ΔU_{int} and ΔF_{int}

The results of ΔU_{int} and ΔF_{int} for BZY10, BZY20, and BZY30 using the long-range interaction model are illustrated in Figure 1, Figure 2, and Figure 3, respectively.

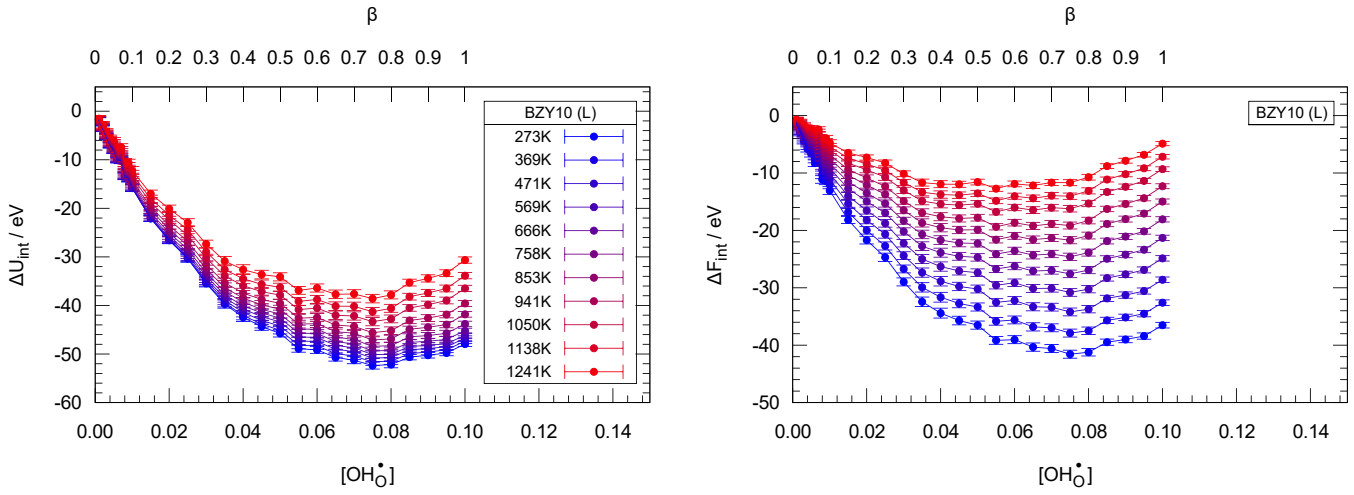

Figure 1. Results of ΔU_{int} and ΔF_{int} for the BZY10 system using the long-range interaction model. Lines are guide to the eye only.

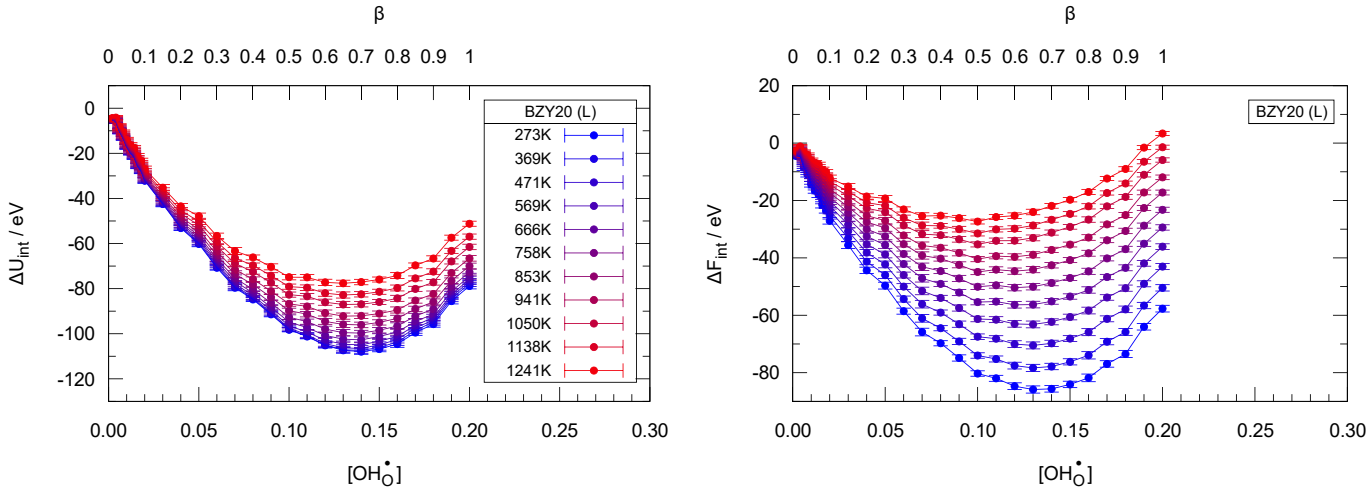

Figure 2. Results of ΔU_{int} and ΔF_{int} for the BZY20 system using the long-range interaction model. Lines are guide to the eye only.

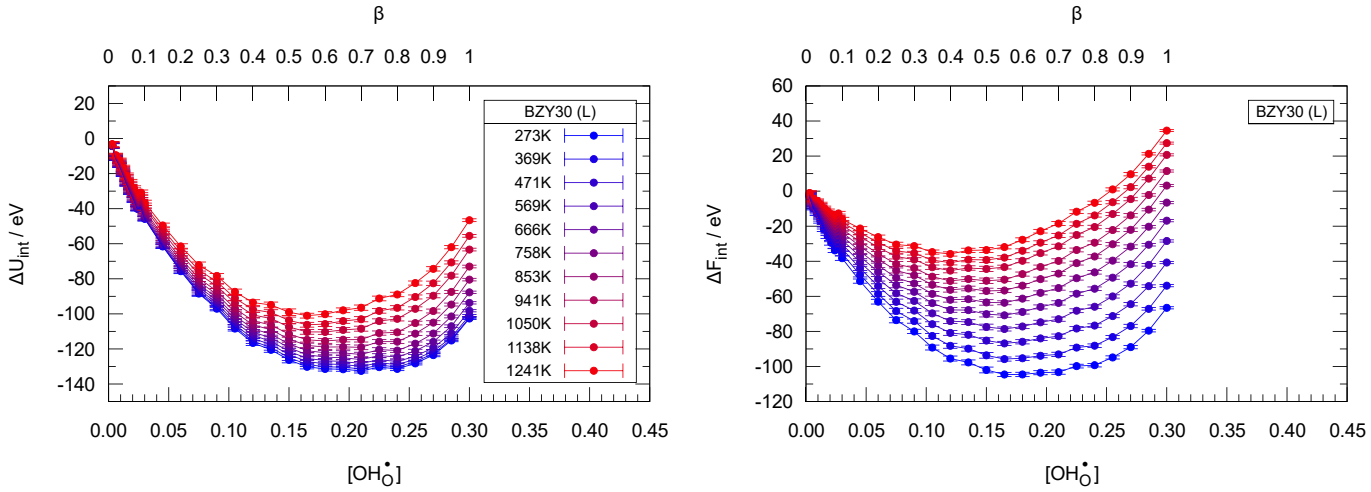

Figure 3. Results of ΔU_{int} and ΔF_{int} for the BZY30 system using the long-range interaction model. Lines are guide to the eye only.

4.2 Results for $\Delta F'_{int}$ and K_{int}

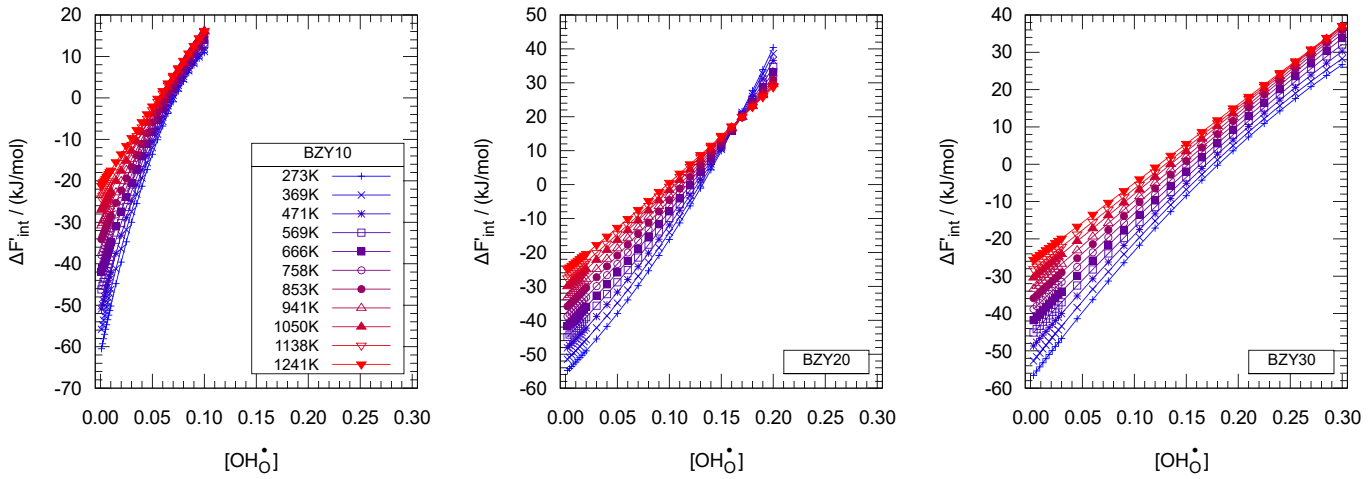

Figure 4. Results of $\Delta F'_{\mathrm{int}}$ for the BZY10 (left), BZY20 (middle), and BZY30 (right) system using the long-range interaction model. Lines are guide to the eye only.

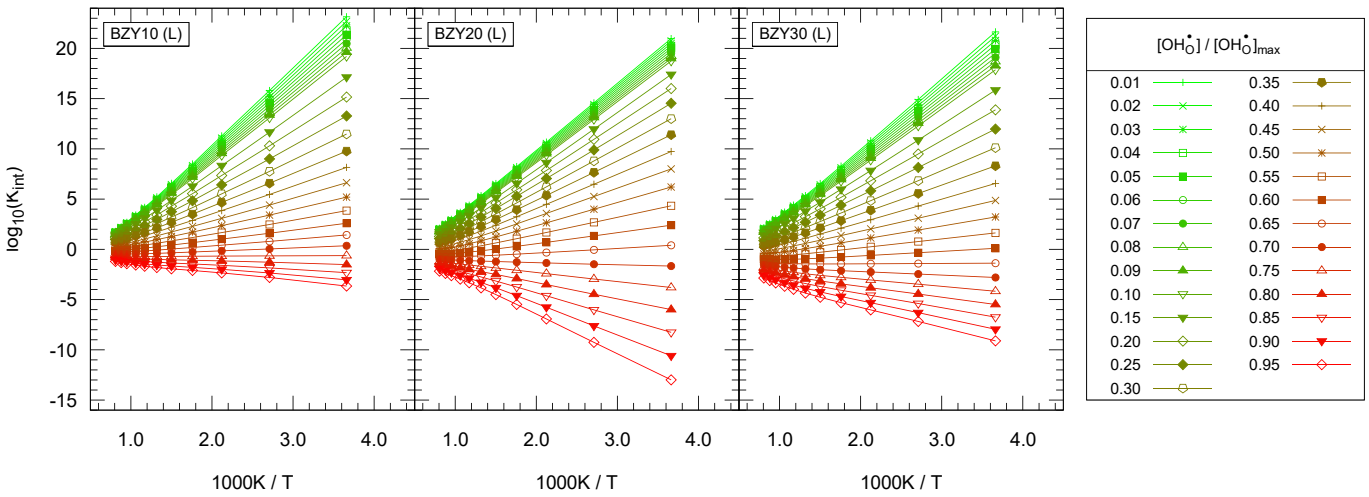

Figure 5. Results of K_{int} for the BZY10 (left), BZY20 (middle), and BZY30 (right) system using the long-range interaction model. Lines are guide to the eye only.

The results of $\Delta F'_{\mathrm{int}}$ and K_{int} for BZY10, BZY20, and BZY30 using the long-range interaction model are illustrated in Figure 4 and Figure 5.

4.3 Results for $[OH^{\bullet}_{O}]$ against p_{H_2O}

The results of $[\mathrm{OH}^{\bullet}_{\mathrm{O}}](p_{\mathrm{H_2O}})$ for BZY10, BZY20, and BZY30 using the long-range interaction model are illustrated in Figure 6.

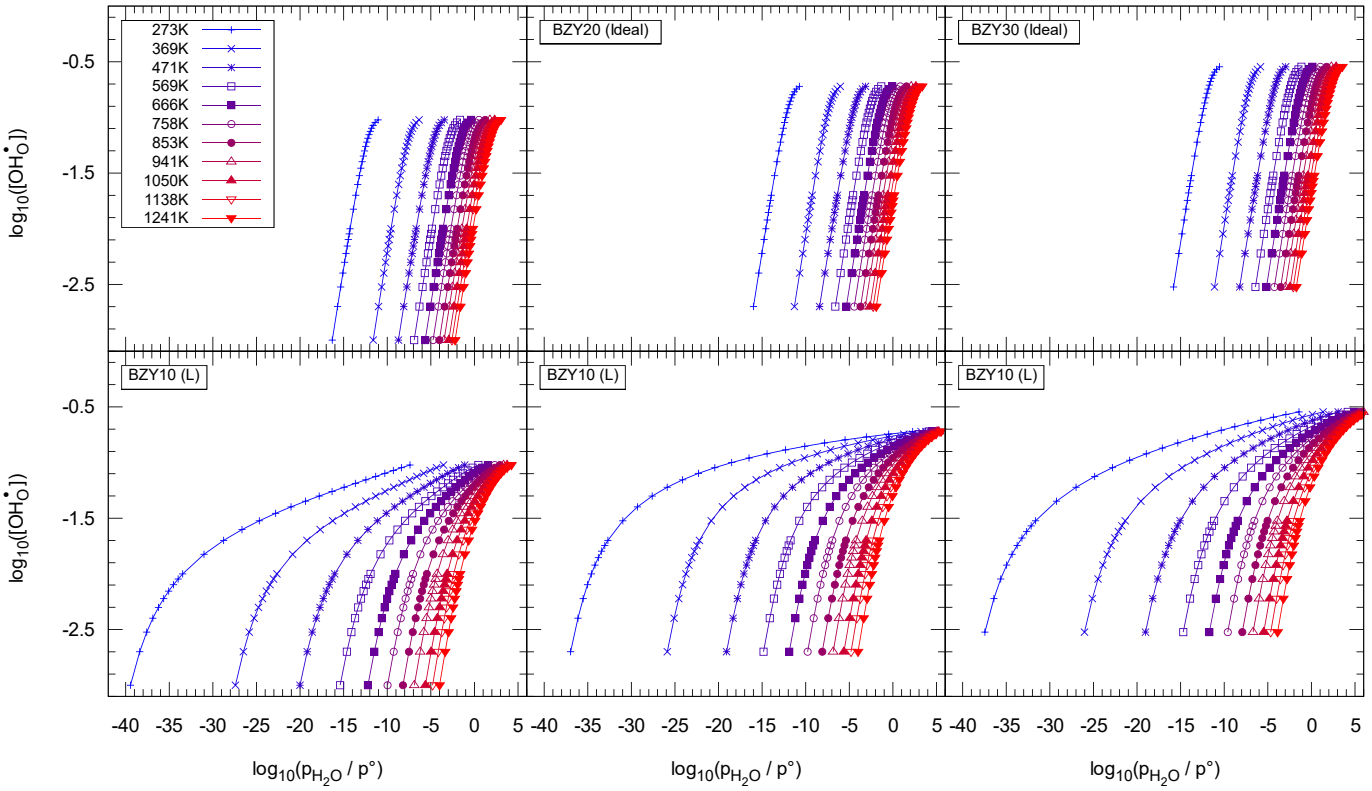

Figure 6. Illustration of $[\mathrm{OH}^{\bullet}_{\mathrm{O}}]$ against $p_{\mathrm{H_2O}}$ for BZY10 (left), BZY20 (middle), and BZY30 (right) using idealized data calculated with $\Delta s°, \Delta h°$ (top) compared to the non-ideal curves after post-processing with the K_{int} datasets (bottom) for the long-range model. Lines are guide to the eye only.

5 Derivation of the mass action law with K_{int}

Please note that the given derivation of the K_{int} formalism uses the incorporation of one $[\mathrm{OH}_{\mathrm{O}}^{\bullet}]$ defect according to the incorporation reaction:

$$\mathrm{v}_{\mathrm{O}}^{\bullet\bullet} + \frac{1}{2}\mathrm{O}_{\mathrm{O}}^{\mathrm{x}} + \frac{1}{2}\mathrm{H_2O} \rightleftharpoons \mathrm{OH}_{\mathrm{O}}^{\bullet}$$

In contrast, the hydration reaction in the main manuscript is normalized to two $[\mathrm{OH}_{\mathrm{O}}^{\bullet}]$ defects as this is the usually used reaction formalism in the literature. The resulting description is equivalent and is normalized to two defects in the last step.

The change in Gibbs free energy of the yttrium-doped barium zirconate system due to the hydration process as written in reaction (2) of the main manuscript $\Delta G(T, N_{\mathrm{Y}}, N_{\mathrm{v}}, N_{\mathrm{H}}, N_{\mathrm{O,hyd}}, N_{\mathrm{H_2O}}, \mu_{\mathrm{H_2O}})$ is a function of temperature T, the number of yttrium ions N_{Y}, the number of oxygen vacancies N_{v}, the number of oxygen vacancies due to the yttrium doping $N_{\mathrm{v,dop}}$, the number of proton defects N_{H}, the number of reintroduced oxygen ions due to hydration $N_{\mathrm{O,hyd}}$, the number of water molecules in the gas phase $N_{\mathrm{H_2O}}$, and the chemical potential of the water gas $\mu_{\mathrm{H_2O}}$. Additional quantities in the formalism are the number of oxygen sites in the system $N_{\mathrm{O,tot}}$, the number of B sites in the system $N_{\mathrm{B,tot}}$, the mixing entropy ΔS_{mix}, and the Gibbs energies of formation for non-interacting defects off oxygen vacancies g_{v}° and protonic defects g_{H}°. The last quantity $\Delta G_{\mathrm{int}}(T, N_{\mathrm{v}}, N_{\mathrm{H}}, N_{\mathrm{Y}})$ describes the influence of interactions between oxygen vacancies, interstitial protons, and yttrium doping on the Gibbs free energy. The value $\Delta G(T, N_{\mathrm{Y}}, N_{\mathrm{v}}, N_{\mathrm{H}}, N_{\mathrm{O,hyd}}, N_{\mathrm{H_2O}}, \mu_{\mathrm{H_2O}})$ is then described according to eq. (1).

$$\Delta G\big(T, N_{\mathrm{Y}}, N_{\mathrm{v}}, N_{\mathrm{H}}, N_{\mathrm{O,hyd}}, N_{\mathrm{H_2O}}, \mu_{\mathrm{H_2O}}\big) = N_{\mathrm{v}} g_{\mathrm{v}}^{\circ} + N_{\mathrm{H}} g_{\mathrm{H}}^{\circ} + N_{\mathrm{H_2O}} \mu_{\mathrm{H_2O}} - T\Delta S_{\mathrm{mix}} + \Delta G_{\mathrm{int}}(T, N_{\mathrm{v}}, N_{\mathrm{H}}, N_{\mathrm{Y}}) \tag{1}$$

The ideal mixing entropy can be described using statistical mechanics. The only relevant contribution in this context is the change in the mixing entropy of the oxygen sublattice as the mixing entropy of the cation lattices does not change due to hydration. Two subcontributions can be distinguished; the first is the mixing entropy of the hydrated system as described by eq. (2).

$$\Delta S_{\mathrm{mix}}^{\mathrm{hyd}}(N_{\mathrm{v,dop}}, N_{\mathrm{O,hyd}}, N_{\mathrm{v}}, N_{\mathrm{H}}) = k_{\mathrm{B}} \ln\left(\frac{(N_{\mathrm{O,tot}})!}{(N_{\mathrm{O,tot}} - N_{\mathrm{v,dop}} - N_{\mathrm{O,hyd}})!\,(N_{\mathrm{H}})!\,(N_{\mathrm{v}})!}\right) \tag{2}$$

The second subcontribution according to eq. (3) is negative and corrects the mixing entropy already present in the dry doped system.

$$\Delta S_{\mathrm{mix}}^{\mathrm{dry}}(N_{\mathrm{v,dop}}, N_{\mathrm{v}}) = -k_{\mathrm{B}} \ln\left(\frac{(N_{\mathrm{O,tot}})!}{(N_{\mathrm{O,tot}} - N_{\mathrm{v,dop}})!\,(N_{\mathrm{v,dop}})!}\right) \tag{3}$$

By introducing several mass balance and charge balance rules according to eq. (4) to eq. (7), eq. (2) and eq. (3) can now be rewritten as eq. (8) and eq. (9), respectively.

$$2\,N_{\mathrm{O,hyd}} = N_{\mathrm{H}} = 2\,N_{\mathrm{H_2O}} \tag{4}$$

$$N_{\mathrm{O,tot}} = 3\,N_{\mathrm{BZO}} \tag{5}$$

$$N_{\mathrm{v}} = N_{\mathrm{v,dop}} - N_{\mathrm{O,hyd}} \tag{6}$$

$$2\,N_{\mathrm{v,dop}} = N_{\mathrm{Y}} \tag{7}$$

$$\Delta S_{\mathrm{mix}}^{\mathrm{hyd}}(N_{\mathrm{Y}}, N_{\mathrm{H}}) = k_{\mathrm{B}} \ln\left(\frac{(3\,N_{\mathrm{BZO}})!}{(3\,N_{\mathrm{BZO}} - 0.5\,N_{\mathrm{Y}} - 0.5\,N_{\mathrm{H}})!\,(N_{\mathrm{H}})!\,(0.5\,N_{\mathrm{Y}} - 0.5\,N_{\mathrm{H}})!}\right) \tag{8}$$

$$\Delta S_{\mathrm{mix}}^{\mathrm{dry}}(N_{\mathrm{Y}}) = -k_{\mathrm{B}} \ln\left(\frac{(3\,N_{\mathrm{BZO}})!}{(3\,N_{\mathrm{BZO}} - 0.5\,N_{\mathrm{Y}})!\,(0.5\,N_{\mathrm{Y}})!}\right) \tag{9}$$

This allows to rewrite eq. (1) as $\Delta G(T, N_\mathrm{Y}, N_\mathrm{H}, \mu_{\mathrm{H_2O}})$ and reduce the interaction contribution to $\Delta G_\mathrm{int}(T, N_\mathrm{H}, N_\mathrm{Y})$ as shown in eq (10). Here, $\Delta_r g$ is the Gibbs energy of the hydration reaction.

$$\Delta G\big(T, N_\mathrm{Y}, N_\mathrm{H}, \mu_{\mathrm{H_2O}}\big) = 0.5\, N_\mathrm{Y} g_\mathrm{v}^\circ + \underbrace{\big(g_\mathrm{H}^\circ - 0.5\, g_\mathrm{v}^\circ + 0.5\, \mu_{\mathrm{H_2O}}\big)}_{\Delta_r g} N_\mathrm{H} - T\Delta S_\mathrm{mix}^\mathrm{hyd}(N_\mathrm{Y}, N_\mathrm{H}) + T\Delta S_\mathrm{mix}^\mathrm{dry}(N_\mathrm{Y}) + \Delta G_\mathrm{int}(T, N_\mathrm{H}, N_\mathrm{Y}) \quad (10)$$

Using the Stirling approximation as shown in eq. (11), the value $\Delta G\big(T, N_\mathrm{Y}, N_\mathrm{H}, \mu_{\mathrm{H_2O}}\big)$ can be minimized with respect to the protonic defects created by hydration which yields eq. (12).

$$\ln(m!) \approx m \ln m - m \quad (11)$$

$$\frac{\partial \Delta G\big(T, N_\mathrm{Y}, N_\mathrm{H}, \mu_{\mathrm{H_2O}}\big)}{\partial N_\mathrm{H}} = \Delta_r g + k_\mathrm{B} T \ln\left(\frac{N_\mathrm{H}}{(3\, N_\mathrm{BZO} - 0.5\, N_\mathrm{Y} - 0.5\, N_\mathrm{H})^{\frac{1}{2}} (0.5\, N_\mathrm{Y} - 0.5\, N_\mathrm{H})^{\frac{1}{2}}}\right) + \frac{\partial \Delta G_\mathrm{int}(T, N_\mathrm{H}, N_\mathrm{Y})}{\partial N_\mathrm{H}} \equiv 0 \quad (12)$$

Reintroducing the lattice molar fractions as described by eq. (13), (14), and (15) yields eq. (16).

$$[\mathrm{O}_\mathrm{O}^\mathrm{x}] = \frac{3\, N_\mathrm{BZO} - 0.5\, N_\mathrm{Y} - 0.5\, N_\mathrm{OH}}{N_\mathrm{BZO}} \quad (13)$$

$$[\mathrm{OH}_\mathrm{O}^\bullet] = \frac{N_\mathrm{OH}}{N_\mathrm{BZO}} \quad (14)$$

$$[\mathrm{v}_\mathrm{O}^{\bullet\bullet}] = \frac{0.5\, N_\mathrm{Y} - 0.5\, N_\mathrm{OH}}{N_\mathrm{BZO}} \quad (15)$$

$$\frac{\partial \Delta G\big(T, N_\mathrm{Y}, N_\mathrm{H}, \mu_{\mathrm{H_2O}}\big)}{\partial N_\mathrm{H}} = \Delta_r g + k_\mathrm{B} T \ln\left(\frac{[\mathrm{OH}_\mathrm{O}^\bullet]}{[\mathrm{O}_\mathrm{O}^\mathrm{x}]^{\frac{1}{2}} [\mathrm{v}_\mathrm{O}^{\bullet\bullet}]^{\frac{1}{2}}}\right) + \underbrace{\frac{\partial \Delta G_\mathrm{int}(T, N_\mathrm{H}, N_\mathrm{Y})}{\partial N_\mathrm{H}}}_{\Delta G'_\mathrm{int}} \equiv 0 \quad (16)$$

Rearranging eq. (16) and reintroducing $\Delta G'_\mathrm{int}$ yields eq. (17).

$$\frac{[\mathrm{OH}_\mathrm{O}^\bullet]}{[\mathrm{O}_\mathrm{O}^\mathrm{x}]^{\frac{1}{2}} [\mathrm{v}_\mathrm{O}^{\bullet\bullet}]^{\frac{1}{2}}} = \exp\left(-\frac{\Delta_r g}{k_\mathrm{B} T}\right) \exp\left(-\frac{\Delta G'_\mathrm{int}}{k_\mathrm{B} T}\right) \quad (17)$$

By further introducing the relation between the reaction free enthalpy $\Delta_r g$ and the standard reaction free enthalpy $\Delta_r g^\circ$ using the standard chemical potential of water vapor $\mu_{\mathrm{H_2O}}^\circ$ as shown in eq. (18), expression (19) can be derived.

$$\Delta_r g = \underbrace{g_\mathrm{H}^\circ - 0.5\, g_\mathrm{v}^\circ + 0.5\, \mu_{\mathrm{H_2O}}^\circ}_{\Delta_r g^\circ} + k_\mathrm{B} T \ln\left(\left(\frac{p_{\mathrm{H_2O}}}{p^\circ}\right)^{-\frac{1}{2}}\right) \quad (18)$$

$$\frac{[\mathrm{OH}_\mathrm{O}^\bullet]}{[\mathrm{O}_\mathrm{O}^\mathrm{x}]^{\frac{1}{2}} [\mathrm{v}_\mathrm{O}^{\bullet\bullet}]^{\frac{1}{2}}} \cdot \left(\frac{1}{p_{\mathrm{H_2O}}}\right)^{\frac{1}{2}} = \exp\left(-\frac{\Delta_r g^\circ}{k_\mathrm{B} T}\right) \exp\left(-\frac{\Delta G'_\mathrm{int}}{k_\mathrm{B} T}\right) = K_0^\mathrm{single}(T) \cdot K_\mathrm{int}^\mathrm{single}(T, N_\mathrm{H}, N_\mathrm{Y}) \quad (19)$$

Squaring eq. (19) to match the more common formalism used in literature, where $K_0(T)$ is given for the reaction with two $\mathrm{OH}_\mathrm{O}^\bullet$ defects, leads to the final expression (20) as used for the calculations of the main manuscript, with $\Delta G^\circ = 2 \cdot \Delta_r g^\circ$, $\sqrt{K_\mathrm{int}} = K_\mathrm{int}^\mathrm{single}$, and $\sqrt{K_0} = K_0^\mathrm{single}$.

$$\frac{[\mathrm{OH}_\mathrm{O}^\bullet]}{[\mathrm{O}_\mathrm{O}^\mathrm{x}][\mathrm{v}_\mathrm{O}^{\bullet\bullet}]} \cdot \frac{1}{p_{\mathrm{H_2O}}} = \exp\left(-\frac{\Delta G^\circ}{k_\mathrm{B} T}\right) \exp\left(-\frac{2 \cdot \Delta G'_\mathrm{int}}{k_\mathrm{B} T}\right) = K_0(T) \cdot K_\mathrm{int}(T, N_\mathrm{H}, N_\mathrm{Y}) \quad (20)$$

6 Obtaining F_{int} from MMC distribution samples

The free energy of a system can be calculated from the canonical partition function Z as shown in (21) where Z is defined according to expression (22).

$$F = -k_{\mathrm{B}}T \cdot \ln(Z) \tag{21}$$

$$Z = \int \Omega(E) \cdot \exp\left(-\frac{E}{k_{\mathrm{B}}T}\right) \mathrm{d}E \tag{22}$$

Here, the quantity $\Omega(E)$ describes the total number of states with energy E. Using the Metropolis Monte Carlo algorithm, it is possible to obtain samples of state distributions $M(E,T)$ that fulfill relation (23).

$$m \cdot M(E,T) = \Omega(E) \cdot \exp\left(-\frac{E}{k_{\mathrm{B}}T}\right) \tag{23}$$

The direct evaluation of Z and consequently F is not possible as the proportionality factor m is unknown. When taking a uniform random sample $\Omega'(E)$ of the configurational space using MMC, that is, a simulation where each exchange attempt is performed without checking the probability function, the equality relation (24) must however hold true as the ration ϑ between $\Omega(E)$ and $\Omega'(E)$ does not depend on the energy E.

$$\frac{\Omega(E)}{\Omega'(E)} = \frac{\int \Omega(E)\mathrm{d}E}{\int \Omega'(E)\mathrm{d}E} = \vartheta \tag{24}$$

Combining equations (24) and (23) yields the relation between the random sample $\Omega'(E)$ and the finite temperature MMC distribution $M(E,T)$ as shown in expression (25).

$$m \cdot M(E) = \vartheta \cdot \Omega'(E) \cdot \exp\left(-\frac{E}{k_{\mathrm{B}}T}\right) \tag{25}$$

Rearranging and integrating the distributions leads to a new factor m' as shown in (26).

$$m' = \frac{m}{\vartheta} = \frac{\int \Omega'(E) \cdot \exp\left(-\frac{E}{k_{\mathrm{B}}T}\right) \mathrm{d}E}{\int M(E,T)\mathrm{d}E} \tag{26}$$

Assuming $\Omega'(E)$ and $M(E,T)$ contain the same number of state samples, the partition function Z can be rewritten into equation (27) where Θ is the total number of configurations of the system as defined in expression (28).

$$Z = m \cdot \int M(E)\mathrm{d}E = m' \cdot \Theta \tag{27}$$

$$\Theta = \int \Omega(E)\mathrm{d}E \tag{28}$$

This allows to redefine the free energy F as shown in (29) where the first term on the right-hand side is the free energy of the ideal system $F(\Theta)$ and the second term is the interaction contribution F_{int}.

$$F = -k_{\mathrm{B}}T \cdot \ln(\Theta) - k_{\mathrm{B}}T \cdot \ln(m') \tag{29}$$

Consequently, the free energy of interaction F_{int} is calculated by rearranging (29) into expression (30).

$$F_{\mathrm{int}} = F - F(\Theta) = -k_{\mathrm{B}}T \cdot \ln(m') \tag{30}$$

Again, the direct evaluation of m' is usually not possible as it rarely possible to obtain $\Omega'(E)$ and $M(E,T)$ that show a statistically significant overlap. At this point, the multistage sampling solution suggested by Valleau and Card[2] that calculates m' from a series of bridging distributions with small temperature deltas as shown in the main manuscript can be used. This additionally solves an issue that m' might be large, causing issues with the standard IEEE754 double precision numbers.

The $\Delta F'_{int}$ raw data

Table 7. The $\Delta F'_{int}$ raw data for proton fraction $[OH^{\bullet}_{O}]$ against temperature calculated from the BZY10 simulations using the short-range interaction model. All values are given in kJ / mol.

$[OH^{\bullet}_{O}]$	273 K	369 K	471 K	666 K	569 K	758 K	853 K	941 K	1050 K	1138 K	1241 K
0.001	-55.2	-51.0	-46.7	-42.7	-39.0	-35.6	-32.3	-29.4	-26.1	-23.7	-21.0
0.002	-54.5	-50.4	-46.1	-42.2	-38.5	-35.1	-31.9	-29.1	-25.8	-23.4	-20.7
0.003	-53.7	-49.7	-45.5	-41.6	-38.0	-34.7	-31.5	-28.7	-25.5	-23.1	-20.5
0.004	-53.0	-49.0	-44.9	-41.1	-37.5	-34.2	-31.1	-28.3	-25.2	-22.8	-20.3
0.005	-52.3	-48.4	-44.3	-40.5	-37.0	-33.8	-30.7	-28.0	-24.9	-22.5	-20.0
0.006	-51.6	-47.7	-43.6	-39.9	-36.5	-33.3	-30.3	-27.6	-24.5	-22.2	-19.8
0.007	-50.9	-47.0	-43.0	-39.4	-35.9	-32.9	-29.9	-27.2	-24.2	-22.0	-19.5
0.008	-50.2	-46.3	-42.4	-38.8	-35.4	-32.4	-29.5	-26.9	-23.9	-21.7	-19.2
0.009	-49.5	-45.7	-41.8	-38.3	-34.9	-31.9	-29.0	-26.5	-23.6	-21.4	-19.0
0.010	-48.8	-45.0	-41.2	-37.7	-34.4	-31.5	-28.6	-26.1	-23.2	-21.1	-18.7
0.015	-45.2	-41.7	-38.1	-34.9	-31.9	-29.2	-26.6	-24.3	-21.6	-19.6	-17.4
0.020	-41.7	-38.4	-35.1	-32.2	-29.4	-26.9	-24.5	-22.4	-19.9	-18.1	-16.1
0.025	-38.2	-35.2	-32.1	-29.4	-26.9	-24.6	-22.4	-20.5	-18.3	-16.6	-14.8
0.030	-34.7	-31.9	-29.1	-26.7	-24.4	-22.4	-20.4	-18.6	-16.6	-15.0	-13.4
0.035	-31.3	-28.7	-26.2	-24.0	-21.9	-20.1	-18.3	-16.7	-14.8	-13.5	-12.0
0.040	-27.8	-25.5	-23.3	-21.3	-19.5	-17.8	-16.2	-14.7	-13.1	-11.9	-10.5
0.045	-24.4	-22.3	-20.4	-18.6	-17.0	-15.5	-14.1	-12.8	-11.3	-10.2	-9.0
0.050	-21.0	-19.2	-17.5	-16.0	-14.5	-13.2	-11.9	-10.8	-9.5	-8.6	-7.5
0.055	-17.6	-16.1	-14.6	-13.3	-12.1	-10.9	-9.8	-8.8	-7.7	-6.9	-6.0
0.060	-14.2	-13.0	-11.8	-10.7	-9.7	-8.7	-7.7	-6.8	-5.9	-5.2	-4.4
0.065	-10.9	-9.9	-9.0	-8.1	-7.2	-6.4	-5.5	-4.8	-4.0	-3.5	-2.9
0.070	-7.5	-6.9	-6.2	-5.5	-4.8	-4.1	-3.4	-2.8	-2.1	-1.7	-1.2
0.075	-4.2	-3.9	-3.5	-3.0	-2.4	-1.8	-1.2	-0.8	-0.2	0.1	0.4
0.080	-0.9	-0.9	-0.7	-0.4	0.0	0.5	0.9	1.3	1.7	1.9	2.1
0.085	2.4	2.1	2.0	2.1	2.4	2.8	3.1	3.4	3.6	3.7	3.8
0.090	5.7	5.0	4.6	4.6	4.8	5.0	5.3	5.5	5.6	5.6	5.5
0.095	9.0	8.0	7.3	7.1	7.2	7.3	7.5	7.6	7.6	7.5	7.3
0.100	12.2	10.8	9.9	9.6	9.5	9.6	9.7	9.7	9.6	9.4	9.1

Table 8. The $\Delta F'_{int}$ raw data for proton fraction $[OH^{\bullet}_{O}]$ against temperature calculated from the BZY20 simulations using the short-range interaction model. All values are given in kJ / mol.

$[OH^{\bullet}_{O}]$	273 K	369 K	471 K	666 K	569 K	758 K	853 K	941 K	1050 K	1138 K	1241 K
0.002	-59.1	-55.7	-52.2	-48.9	-45.7	-42.6	-39.6	-36.9	-33.7	-31.4	-28.7
0.004	-58.5	-55.2	-51.7	-48.4	-45.1	-42.1	-39.1	-36.4	-33.3	-30.9	-28.3
0.006	-58.0	-54.6	-51.1	-47.8	-44.6	-41.6	-38.6	-35.9	-32.8	-30.5	-27.9
0.008	-57.4	-54.1	-50.6	-47.3	-44.0	-41.1	-38.1	-35.5	-32.4	-30.1	-27.6
0.010	-56.8	-53.5	-50.0	-46.7	-43.5	-40.5	-37.6	-35.0	-31.9	-29.7	-27.2
0.012	-56.3	-52.9	-49.5	-46.2	-43.0	-40.0	-37.1	-34.5	-31.5	-29.2	-26.8
0.014	-55.7	-52.4	-48.9	-45.6	-42.4	-39.5	-36.6	-34.0	-31.1	-28.8	-26.4
0.016	-55.1	-51.8	-48.3	-45.0	-41.9	-38.9	-36.1	-33.5	-30.6	-28.4	-26.0
0.018	-54.5	-51.2	-47.7	-44.5	-41.3	-38.4	-35.6	-33.1	-30.1	-28.0	-25.6

0.020	-53.9	-50.6	-47.2	-43.9	-40.8	-37.9	-35.1	-32.6	-29.7	-27.5	-25.2
0.030	-50.9	-47.6	-44.2	-41.0	-38.0	-35.2	-32.5	-30.1	-27.4	-25.4	-23.2
0.040	-47.7	-44.5	-41.2	-38.0	-35.1	-32.5	-29.9	-27.7	-25.1	-23.2	-21.2
0.050	-44.3	-41.2	-38.0	-35.0	-32.2	-29.7	-27.3	-25.2	-22.8	-21.0	-19.1
0.060	-40.9	-37.9	-34.8	-31.9	-29.3	-26.9	-24.6	-22.7	-20.5	-18.8	-17.1
0.070	-37.2	-34.4	-31.5	-28.8	-26.3	-24.0	-21.9	-20.1	-18.1	-16.6	-15.0
0.080	-33.5	-30.8	-28.1	-25.5	-23.2	-21.2	-19.2	-17.6	-15.7	-14.4	-12.9
0.090	-29.5	-27.1	-24.6	-22.3	-20.1	-18.2	-16.5	-15.0	-13.3	-12.1	-10.8
0.100	-25.5	-23.3	-21.0	-18.9	-17.0	-15.3	-13.7	-12.4	-10.9	-9.8	-8.7
0.110	-21.3	-19.3	-17.3	-15.5	-13.8	-12.3	-10.9	-9.7	-8.5	-7.5	-6.5
0.120	-16.9	-15.3	-13.5	-12.0	-10.5	-9.2	-8.1	-7.1	-6.0	-5.2	-4.4
0.130	-12.4	-11.1	-9.7	-8.4	-7.2	-6.2	-5.2	-4.4	-3.5	-2.9	-2.2
0.140	-7.8	-6.8	-5.7	-4.8	-3.9	-3.1	-2.3	-1.7	-1.0	-0.5	0.0
0.150	-3.0	-2.3	-1.7	-1.1	-0.5	0.1	0.6	1.1	1.5	1.9	2.2
0.160	1.9	2.2	2.4	2.7	3.0	3.3	3.6	3.8	4.1	4.3	4.4
0.170	7.0	6.8	6.7	6.5	6.5	6.5	6.6	6.6	6.7	6.7	6.7
0.180	12.2	11.6	11.0	10.4	10.0	9.8	9.6	9.4	9.3	9.1	8.9
0.190	17.5	16.5	15.4	14.4	13.6	13.1	12.6	12.3	11.9	11.6	11.2
0.200	23.0	21.5	19.9	18.4	17.3	16.4	15.7	15.1	14.5	14.0	13.5

Table 9. The $\Delta F'_{\text{int}}$ raw data for proton fraction $[OH^{\bullet}_{O}]$ against temperature calculated from the BZY30 simulations using the short-range interaction model. All values are given in kJ / mol.

$[OH^{\bullet}_{O}]$	273 K	369 K	471 K	666 K	569 K	758 K	853 K	941 K	1050 K	1138 K	1241 K
0.003	-60.5	-56.7	-52.8	-49.4	-46.2	-43.4	-40.7	-38.3	-35.5	-33.4	-31.0
0.006	-59.6	-55.9	-52.1	-48.7	-45.6	-42.8	-40.1	-37.8	-35.0	-32.9	-30.6
0.009	-58.8	-55.1	-51.4	-48.1	-45.0	-42.2	-39.6	-37.2	-34.5	-32.5	-30.1
0.012	-58.0	-54.3	-50.7	-47.4	-44.4	-41.6	-39.0	-36.7	-34.0	-32.0	-29.7
0.015	-57.1	-53.6	-50.0	-46.7	-43.7	-41.1	-38.5	-36.2	-33.5	-31.5	-29.2
0.018	-56.3	-52.8	-49.3	-46.1	-43.1	-40.5	-37.9	-35.7	-33.0	-31.0	-28.8
0.021	-55.5	-52.0	-48.6	-45.4	-42.5	-39.9	-37.4	-35.1	-32.5	-30.6	-28.3
0.024	-54.7	-51.3	-47.9	-44.8	-41.9	-39.3	-36.8	-34.6	-32.0	-30.1	-27.9
0.027	-53.9	-50.5	-47.2	-44.1	-41.3	-38.7	-36.2	-34.1	-31.5	-29.6	-27.4
0.030	-53.0	-49.8	-46.4	-43.4	-40.6	-38.1	-35.7	-33.5	-31.0	-29.1	-27.0
0.045	-49.0	-46.0	-42.9	-40.1	-37.5	-35.2	-32.9	-30.8	-28.5	-26.7	-24.7
0.060	-45.0	-42.2	-39.4	-36.8	-34.4	-32.2	-30.0	-28.1	-25.9	-24.2	-22.4
0.075	-41.0	-38.4	-35.9	-33.5	-31.3	-29.2	-27.2	-25.4	-23.3	-21.8	-20.1
0.090	-37.1	-34.7	-32.4	-30.2	-28.1	-26.2	-24.3	-22.7	-20.7	-19.3	-17.7
0.105	-33.2	-31.0	-28.9	-26.9	-24.9	-23.2	-21.4	-19.9	-18.1	-16.8	-15.3
0.120	-29.3	-27.4	-25.4	-23.5	-21.8	-20.1	-18.5	-17.1	-15.5	-14.3	-12.9
0.135	-25.5	-23.7	-21.9	-20.2	-18.6	-17.1	-15.6	-14.3	-12.8	-11.7	-10.5
0.150	-21.7	-20.1	-18.5	-16.9	-15.4	-14.0	-12.7	-11.5	-10.1	-9.1	-8.1
0.165	-18.0	-16.5	-15.0	-13.6	-12.2	-10.9	-9.7	-8.6	-7.4	-6.6	-5.6
0.180	-14.3	-13.0	-11.6	-10.3	-9.0	-7.8	-6.7	-5.7	-4.7	-3.9	-3.2
0.195	-10.7	-9.4	-8.2	-6.9	-5.8	-4.7	-3.7	-2.8	-1.9	-1.3	-0.7
0.210	-7.1	-5.9	-4.7	-3.6	-2.5	-1.5	-0.7	0.1	0.8	1.4	1.9
0.225	-3.5	-2.4	-1.3	-0.3	0.7	1.6	2.4	3.0	3.6	4.0	4.4

0.240	0.0	1.0	2.1	3.1	4.0	4.8	5.5	6.0	6.5	6.7	7.0
0.255	3.5	4.5	5.4	6.4	7.3	8.0	8.6	9.0	9.3	9.5	9.6
0.270	7.0	7.9	8.8	9.7	10.5	11.2	11.7	12.0	12.2	12.2	12.2
0.285	10.4	11.2	12.2	13.1	13.8	14.4	14.8	15.0	15.0	15.0	14.8
0.300	13.7	14.6	15.5	16.4	17.1	17.7	18.0	18.1	18.0	17.8	17.4

Table 10. The $\Delta F'_{\text{int}}$ raw data for proton fraction $[OH^{\bullet}_{O}]$ against temperature calculated from the BZY10 simulations using the long-range interaction model. All values are given in kJ / mol.

$[OH^{\bullet}_{O}]$	273 K	369 K	471 K	666 K	569 K	758 K	853 K	941 K	1050 K	1138 K	1241 K
0.001	-60.5	-55.8	-50.9	-46.2	-41.9	-37.9	-34.1	-30.8	-27.0	-24.2	-21.2
0.002	-59.3	-54.7	-49.9	-45.3	-41.0	-37.2	-33.4	-30.2	-26.5	-23.7	-20.7
0.003	-58.1	-53.6	-48.9	-44.4	-40.2	-36.5	-32.8	-29.6	-26.0	-23.3	-20.3
0.004	-57.0	-52.5	-47.9	-43.5	-39.4	-35.7	-32.2	-29.0	-25.5	-22.8	-19.9
0.005	-55.8	-51.5	-46.9	-42.7	-38.7	-35.0	-31.5	-28.5	-25.0	-22.4	-19.5
0.006	-54.7	-50.4	-45.9	-41.8	-37.9	-34.3	-30.9	-27.9	-24.5	-21.9	-19.1
0.007	-53.5	-49.3	-45.0	-40.9	-37.1	-33.6	-30.3	-27.3	-24.0	-21.4	-18.7
0.008	-52.4	-48.3	-44.0	-40.1	-36.3	-32.9	-29.6	-26.8	-23.5	-21.0	-18.3
0.009	-51.3	-47.2	-43.1	-39.2	-35.5	-32.2	-29.0	-26.2	-23.0	-20.5	-17.9
0.010	-50.2	-46.2	-42.1	-38.3	-34.8	-31.5	-28.4	-25.6	-22.5	-20.1	-17.5
0.015	-44.8	-41.2	-37.5	-34.2	-31.0	-28.1	-25.3	-22.8	-20.0	-17.9	-15.5
0.020	-39.6	-36.4	-33.1	-30.2	-27.4	-24.8	-22.3	-20.1	-17.6	-15.7	-13.6
0.025	-34.7	-31.8	-28.9	-26.3	-23.9	-21.6	-19.4	-17.4	-15.2	-13.5	-11.6
0.030	-30.0	-27.4	-24.9	-22.6	-20.5	-18.5	-16.6	-14.8	-12.8	-11.3	-9.7
0.035	-25.5	-23.2	-21.0	-19.1	-17.2	-15.5	-13.8	-12.3	-10.5	-9.2	-7.7
0.040	-21.3	-19.3	-17.4	-15.7	-14.1	-12.6	-11.1	-9.8	-8.2	-7.1	-5.8
0.045	-17.3	-15.6	-13.9	-12.4	-11.0	-9.7	-8.5	-7.3	-6.0	-5.0	-3.9
0.050	-13.6	-12.0	-10.6	-9.3	-8.1	-7.0	-5.9	-4.9	-3.8	-3.0	-2.0
0.055	-10.1	-8.7	-7.5	-6.4	-5.4	-4.4	-3.4	-2.6	-1.6	-0.9	-0.2
0.060	-6.8	-5.7	-4.6	-3.6	-2.7	-1.9	-1.0	-0.3	0.5	1.1	1.7
0.065	-3.7	-2.8	-1.9	-1.0	-0.2	0.6	1.3	1.9	2.6	3.1	3.5
0.070	-0.9	-0.1	0.7	1.4	2.2	2.9	3.6	4.1	4.6	5.0	5.4
0.075	1.6	2.3	3.0	3.8	4.5	5.1	5.7	6.2	6.7	6.9	7.2
0.080	4.0	4.5	5.2	5.9	6.6	7.3	7.9	8.3	8.6	8.8	9.0
0.085	6.1	6.5	7.2	7.9	8.7	9.3	9.9	10.3	10.6	10.7	10.7
0.090	7.9	8.3	9.0	9.8	10.6	11.3	11.9	12.2	12.5	12.5	12.5
0.095	9.5	9.9	10.6	11.4	12.4	13.1	13.7	14.1	14.3	14.4	14.3
0.100	10.9	11.2	12.0	13.0	14.0	14.9	15.6	16.0	16.2	16.2	16.0

Table 11. The $\Delta F'_{\text{int}}$ raw data for proton fraction $[OH^{\bullet}_{O}]$ against temperature calculated from the BZY20 simulations using the long-range interaction model. All values are given in kJ / mol.

$[OH^{\bullet}_{O}]$	273 K	369 K	471 K	666 K	569 K	758 K	853 K	941 K	1050 K	1138 K	1241 K
0.002	-54.8	-51.5	-48.1	-44.9	-41.7	-38.8	-35.9	-33.2	-30.0	-27.6	-24.9
0.004	-54.2	-50.9	-47.4	-44.2	-41.1	-38.2	-35.3	-32.6	-29.5	-27.1	-24.4
0.006	-53.6	-50.2	-46.8	-43.6	-40.5	-37.6	-34.6	-32.0	-28.9	-26.5	-23.9
0.008	-52.9	-49.6	-46.2	-43.0	-39.8	-36.9	-34.0	-31.4	-28.4	-26.0	-23.4

0.010	-52.3	-49.0	-45.5	-42.3	-39.2	-36.3	-33.4	-30.8	-27.8	-25.5	-22.9
0.012	-51.6	-48.3	-44.9	-41.7	-38.6	-35.7	-32.8	-30.2	-27.2	-24.9	-22.4
0.014	-51.0	-47.7	-44.2	-41.0	-37.9	-35.1	-32.2	-29.7	-26.7	-24.4	-21.9
0.016	-50.3	-47.0	-43.6	-40.4	-37.3	-34.4	-31.6	-29.1	-26.1	-23.9	-21.4
0.018	-49.6	-46.3	-42.9	-39.7	-36.6	-33.8	-31.0	-28.5	-25.6	-23.3	-20.9
0.020	-49.0	-45.7	-42.3	-39.1	-36.0	-33.2	-30.4	-27.9	-25.0	-22.8	-20.4
0.030	-45.5	-42.2	-38.9	-35.7	-32.7	-29.9	-27.3	-24.9	-22.2	-20.1	-17.8
0.040	-41.8	-38.7	-35.4	-32.3	-29.4	-26.7	-24.1	-21.9	-19.3	-17.4	-15.3
0.050	-38.0	-34.9	-31.7	-28.8	-25.9	-23.4	-20.9	-18.8	-16.4	-14.6	-12.7
0.060	-34.0	-31.1	-28.0	-25.2	-22.5	-20.0	-17.7	-15.7	-13.5	-11.9	-10.1
0.070	-29.8	-27.0	-24.2	-21.5	-18.9	-16.6	-14.5	-12.6	-10.6	-9.1	-7.5
0.080	-25.4	-22.9	-20.2	-17.7	-15.3	-13.2	-11.2	-9.5	-7.6	-6.3	-4.8
0.090	-20.9	-18.6	-16.1	-13.8	-11.6	-9.7	-7.9	-6.4	-4.7	-3.4	-2.1
0.100	-16.2	-14.1	-11.9	-9.8	-7.9	-6.2	-4.5	-3.2	-1.7	-0.6	0.6
0.110	-11.3	-9.5	-7.6	-5.8	-4.1	-2.6	-1.2	0.0	1.4	2.3	3.3
0.120	-6.3	-4.7	-3.1	-1.6	-0.2	1.1	2.3	3.3	4.4	5.2	6.0
0.130	-1.1	0.2	1.4	2.6	3.7	4.7	5.7	6.5	7.5	8.1	8.8
0.140	4.3	5.2	6.1	6.9	7.7	8.5	9.2	9.8	10.5	11.0	11.5
0.150	9.9	10.4	10.9	11.3	11.8	12.2	12.7	13.2	13.7	14.0	14.4
0.160	15.7	15.8	15.8	15.8	15.9	16.1	16.3	16.5	16.8	17.0	17.2
0.170	21.6	21.3	20.8	20.4	20.1	19.9	19.9	19.9	19.9	20.0	20.0
0.180	27.7	26.9	26.0	25.1	24.4	23.9	23.5	23.3	23.1	23.0	22.9
0.190	33.9	32.7	31.2	29.8	28.7	27.8	27.2	26.7	26.3	26.1	25.8
0.200	40.4	38.6	36.6	34.7	33.1	31.9	30.9	30.2	29.6	29.1	28.7

Table 12. The $\Delta F'_{\text{int}}$ raw data for proton fraction $[OH_O^{\bullet}]$ against temperature calculated from the BZY30 simulations using the long-range interaction model. All values are given in kJ / mol.

$[OH_O^{\bullet}]$	273 K	369 K	471 K	666 K	569 K	758 K	853 K	941 K	1050 K	1138 K	1241 K
0.003	-56.6	-52.7	-48.7	-45.1	-41.8	-38.8	-35.9	-33.4	-30.4	-28.1	-25.6
0.006	-55.4	-51.6	-47.7	-44.2	-40.9	-38.0	-35.2	-32.6	-29.7	-27.4	-24.9
0.009	-54.3	-50.6	-46.7	-43.3	-40.0	-37.2	-34.4	-31.9	-29.0	-26.8	-24.3
0.012	-53.2	-49.5	-45.8	-42.3	-39.2	-36.4	-33.6	-31.2	-28.3	-26.1	-23.7
0.015	-52.1	-48.5	-44.8	-41.4	-38.3	-35.5	-32.8	-30.4	-27.6	-25.4	-23.0
0.018	-51.0	-47.5	-43.8	-40.5	-37.5	-34.7	-32.1	-29.7	-26.9	-24.8	-22.4
0.021	-49.9	-46.4	-42.9	-39.6	-36.6	-33.9	-31.3	-29.0	-26.2	-24.1	-21.8
0.024	-48.8	-45.4	-41.9	-38.7	-35.8	-33.1	-30.5	-28.2	-25.5	-23.4	-21.1
0.027	-47.8	-44.4	-41.0	-37.8	-34.9	-32.3	-29.8	-27.5	-24.8	-22.8	-20.5
0.030	-46.7	-43.4	-40.0	-37.0	-34.1	-31.5	-29.0	-26.7	-24.1	-22.1	-19.9
0.045	-41.4	-38.4	-35.3	-32.5	-29.9	-27.5	-25.2	-23.1	-20.6	-18.8	-16.7
0.060	-36.3	-33.5	-30.7	-28.2	-25.8	-23.6	-21.4	-19.4	-17.2	-15.4	-13.5
0.075	-31.3	-28.8	-26.2	-23.9	-21.7	-19.6	-17.6	-15.8	-13.7	-12.1	-10.3
0.090	-26.4	-24.1	-21.8	-19.7	-17.6	-15.7	-13.9	-12.2	-10.3	-8.8	-7.2
0.105	-21.7	-19.6	-17.5	-15.5	-13.6	-11.9	-10.1	-8.6	-6.8	-5.5	-4.0
0.120	-17.1	-15.2	-13.3	-11.5	-9.7	-8.1	-6.4	-5.0	-3.4	-2.2	-0.9
0.135	-12.7	-10.9	-9.1	-7.5	-5.8	-4.3	-2.8	-1.5	0.0	1.1	2.3
0.150	-8.4	-6.8	-5.1	-3.5	-2.0	-0.5	0.9	2.1	3.4	4.4	5.5

0.165	-4.3	-2.7	-1.2	0.4	1.8	3.2	4.5	5.6	6.8	7.7	8.6
0.180	-0.3	1.2	2.7	4.2	5.6	6.9	8.1	9.1	10.2	11.0	11.8
0.195	3.6	5.0	6.5	7.9	9.3	10.5	11.6	12.6	13.6	14.3	15.0
0.210	7.3	8.7	10.1	11.6	12.9	14.1	15.2	16.0	16.9	17.5	18.1
0.225	10.9	12.2	13.7	15.2	16.5	17.7	18.7	19.5	20.3	20.8	21.3
0.240	14.3	15.7	17.2	18.7	20.1	21.2	22.2	22.9	23.6	24.1	24.5
0.255	17.6	19.0	20.6	22.2	23.6	24.7	25.6	26.3	27.0	27.3	27.6
0.270	20.8	22.2	23.9	25.6	27.0	28.2	29.1	29.7	30.3	30.6	30.8
0.285	23.8	25.3	27.1	28.9	30.4	31.6	32.5	33.1	33.6	33.8	33.9
0.300	26.7	28.3	30.3	32.1	33.8	35.0	35.9	36.5	36.9	37.1	37.1

7 References

1 S. Eisele and S. Grieshammer, *Journal of Computational Chemistry*, 2020, **41**, 2663–2677.

2 J. P. Valleau and D. N. Card, *The Journal of Chemical Physics*, 1972, **57**, 5457–5462.